Brazilian Journal of Biometrics, **44**, 1–24 (2026)
doi:10.28951/bjb.v44i3.958

BRAZILIAN JOURNAL OF BIOMETRICS
ISSN:2764-5290

ARTICLE

A flexible reliability and performance modeling framework using the unit inverse Lomax distribution

Shameera T[⋆,1] and Bindu Punathumparambath[⋆,2]

[1]Department of Statistics, MES Mampad College, Malappuram, Kerala, India.
[2]Department of Statistics, Govt. Arts & Science College, Kozhikode, Kerala, India.
[⋆]Corresponding author. Email: shameeranaseerok@gmail.com; ppbindukannan@gmail.com

(Received: August 12, 2025; Revised: January 22, 2026; Accepted: May 20, 2026; Published: September 11, 2026)
Section Editor: Luiz Ricardo Nakamura

Abstract

The Unit Inverse Lomax Distribution (UILxD) is introduced as a new statistical model tailored for data within the unit interval. This paper explores the theoretical framework of UILxD, presenting closed form expressions for its probability density function, cumulative distribution function, survival function, hazard rate, and quantile function. The model's flexibility is highlighted through its ability to capture diverse data characteristics, such as skewness, kurtosis, and heavy tails, making it suitable for applications in fields like insurance, finance, and reliability engineering. Key statistical properties, including moments, mode, order statistics, and various entropy measures are derived. Multiple estimation methods—Maximum Likelihood Estimation, Cramer Von Mises, Ordinary and Weighted Least Squares, and Percentile Estimation are investigated through a Monte Carlo simulation study, demonstrating their performance across different sample sizes. The practical utility of UILxD is validated using three real world datasets , where it outperforms established unit interval distributions based on goodness of fit metrics.
Keywords: Unit inverse Lomax distribution; statistical properties; measures of uncertainty; estimation; simulation study.

1. Introduction

Statistical modeling of continuous random variables constrained to the open unit interval $(0, 1)$ is crucial in various disciplines, including reliability engineering, economics, environmental studies, and medical research. Several models have been developed using the transformation of distributions. Examples include the unit Gamma/Gompertz distribution (Bantan *et al.*, 2021), the unit generalized log Burr–XII distribution (Bhatti *et al.*, 2021), the power unit inverse Lindley distribution (Gemeay *et al.*, 2024), the unit inverse Gaussian distribution (Ghitany *et al.*, 2018), the unit inverse exponentiated Weibull distribution (Hassan & Alharbi, , 2023), the unit Burr–XII distribution (

Korkmaz & Chesnea, 2021), the Kumaraswamy distribution (Kumaraswamy, 1980), the unit Birnbaum Saunders distribution (Mazucheli *et al.*, 2018a), the unit Weibull distribution (Mazucheli *et al.*, 2018b), the unit Lindley distribution (Mazucheli *et al.*, 2019a), the unit Gompertz distribution (Mazucheli *et al.*, 2019b), the unit inverse Weibull distribution (Shameera & Bindu, 2023), and the zero, one and zero-and-one-inflated new unit Lindley distribution (Ferreira & Mazucheli, 2022).

Among the versatile baseline distributions used for such transformations, the Lomax distribution (LxD) stands out for its ability to model heavy tailed phenomena. The p.d.f. of the LxD (Abiodun & Ishaq, 2022) is given by:

$$h(x;\lambda,\beta)=\frac{\lambda}{\beta}\left(1+\frac{x}{\beta}\right)^{-(\lambda+1)},\lambda,\beta>0,x\geq 0.$$

The c.d.f of LxD is,

$$H(x;\lambda,\beta)=1-\left(1+\frac{x}{\beta}\right)^{-\lambda},\lambda,\beta>0,x\geq 0. \tag{1}$$

There are several extensions of the Lomax distribution, including the extended LxD (Lemonte & Cordeiro, 2011), the gamma LxD (Cordeiro *et al.*, 2013), the exponential LxD (Elbassiouny *et al.*, 2012), the weighted LxD (Kilany, 2016), the power LxD (Rady *et al.*, 2016), the inverse LxD (Hassan & Mohamed, 2019), the Weibull LxD (Hassan & Abd-Allah, 2022), and the mixture of Lomax and Gamma Distribution (Sakthivel & Pandiyan, 2025) among others. Due to its versatility and ability to model heavy tailed phenomena, the LxD remains a prominent topic in statistical research.

In this paper, we introduce the unit inverse Lomax distribution (UILxD), present its key statistical characteristics, explore several estimation techniques, conduct a simulation study to evaluate estimator performance, and demonstrate its applicability through analysis of real world datasets.

The p.d.f of two parameter inverse LxD (Hassan & Mohamed, 2019) is,

$$g(x;\lambda,\beta)=\frac{\lambda\beta}{x^2}\left(1+\frac{\beta}{x}\right)^{-(\lambda+1)},x,\lambda,\beta>0. \tag{2}$$

The c.d.f of inverse LxD is,

$$G(x;\lambda,\beta)=\left(1+\frac{\beta}{x}\right)^{-\lambda},x,\lambda,\beta>0. \tag{3}$$

2. Formulation of the Unit Inverse Lomax Distribution

2.1 Derivation and Basic Properties

The Unit Inverse Lomax Distribution (UILxD) is derived through a transformation of the Inverse Lomax random variable. Let $Z\sim$ ILxD(λ,β) with probability density function (PDF) given in (2). The transformation , $X=\frac{1}{1+Z}$ maps the support from $(0,\infty)$ to the unit interval $(0,1)$, yielding the UILxD with the following fundamental functions:

Proposition 1 (Density and Distribution Functions). *The PDF and CDF of UILxD are respectively:*

$$f(x;\lambda,\beta)=\frac{\lambda\beta}{(1-x)^2}\left(1+\frac{\beta x}{1-x}\right)^{-(\lambda+1)},\quad x\in(0,1), \tag{4}$$

$$F(x;\lambda,\beta)=1-\left(1+\frac{\beta x}{1-x}\right)^{-\lambda},\quad x\in(0,1), \tag{5}$$

where $\lambda>0$ is the shape parameter and $\beta>0$ is the scale parameter.

2.2 Boundary Behavior and Special Cases

Proposition 2 (Asymptotic Properties). *The UILxD exhibits distinctive boundary behavior:*

- ***PDF at boundaries:***

$$\lim_{x \to 0^+} f(x; \lambda, \beta) = \lambda\beta,$$
$$\lim_{x \to 1^-} f(x; \lambda, \beta) = +\infty.$$

- ***CDF at boundaries:***

$$\lim_{x \to 0^+} F(x; \lambda, \beta) = 0,$$
$$\lim_{x \to 1^-} F(x; \lambda, \beta) = 1.$$

Proposition 3 (Tail Behavior). *The tail behavior of the pdf of the UILxD is given by:*

- ***Left tail*** *($x \to 0^+$):*
$$f(x) \sim \lambda\beta.$$
- ***Right tail*** *($x \to 1^-$):*
$$f(x) \sim \lambda\beta^{-\lambda}(1-x)^{\lambda-1}.$$

Remark 1. *: The explosive growth of the PDF as $x \to 1^-$ distinguishes UILxD from many common unit interval distributions (e.g., Beta distribution) and makes it particularly suitable for modeling data with accumulation near the upper boundary.*

2.3 Survival and Hazard Characteristics

The UILxD possesses the following important reliability functions:

Proposition 4 (Reliability Functions). *For the UILxD with parameters $\lambda, \beta > 0$:*

- ***Survival function:***

$$S(x; \lambda, \beta) = \left(1 + \frac{\beta x}{1-x}\right)^{-\lambda}. \tag{6}$$

- ***Hazard rate function:***

$$h(x; \lambda, \beta) = \frac{\lambda\beta}{(1-x)(1+(\beta-1)x)} \tag{7}$$

- ***Reversed hazard rate function***

$$\tau(x; \lambda, \beta) = \frac{\lambda\beta}{(1-x)^2\left(1+\frac{\beta x}{1-x}\right)\left[\left(1+\frac{\beta x}{1-x}\right)^{\lambda} - 1\right]} \tag{8}$$

- ***Cumulative hazard function:***

$$H(x; \lambda, \beta) = \lambda \ln\left(1 + \frac{\beta x}{1-x}\right). \tag{9}$$

Proof.

- **Survival function:**
  The survival function is defined as

$$\begin{aligned} S(x;\lambda,\beta) &= 1 - F(x;\lambda,\beta) \\ &= 1 - \left[1 - \left(1 + \frac{\beta x}{1-x}\right)^{-\lambda}\right] \\ &= \left(1 + \frac{\beta x}{1-x}\right)^{-\lambda}. \end{aligned}$$

- **Hazard rate function**
  The hazard rate function is defined as

$$h(x;\lambda,\beta) = \frac{f(x;\lambda,\beta)}{S(x;\lambda,\beta)}$$

$$h(x;\lambda,\beta) = \frac{\lambda\beta}{(1-x)^2\left(1+\frac{\beta x}{1-x}\right)^{-(\lambda+1)}}\left(1+\frac{\beta x}{1-x}\right)^{-\lambda}$$

  Since

$$1 + \frac{\beta x}{1-x} = \frac{1+(\beta-1)x}{1-x},$$

  we obtain

$$h(x;\lambda,\beta) = \frac{\lambda\beta}{(1-x)\left(1+(\beta-1)x\right)}.$$

- **Reversed hazard rate function**
  The reversed hazard rate function is defined as

$$\tau(x;\lambda,\beta) = \frac{f(x;\lambda,\beta)}{F(x;\lambda,\beta)}.$$

$$\begin{aligned} \tau(x;\lambda,\beta) &= \frac{\frac{\lambda\beta}{(1-x)^2}\left(1+\frac{\beta x}{1-x}\right)^{-(\lambda+1)}}{1-\left(1+\frac{\beta x}{1-x}\right)^{-\lambda}} \\ &= \frac{\frac{\lambda\beta}{(1-x)^2}}{\left(1+\frac{\beta x}{1-x}\right)^{\lambda+1}\left[1-\left(1+\frac{\beta x}{1-x}\right)^{-\lambda}\right]} \\ &= \frac{\lambda\beta}{(1-x)^2\left(1+\frac{\beta x}{1-x}\right)\left[\left(1+\frac{\beta x}{1-x}\right)^{\lambda}-1\right]}. \end{aligned}$$

- **Cumulative hazard function:**
  The cumulative hazard function is defined as

$$H(x;\lambda,\beta) = -\ln S(x;\lambda,\beta).$$

$$H(x;\lambda,\beta) = -\ln\left[\left(1+\frac{\beta x}{1-x}\right)^{-\lambda}\right]$$
$$= \lambda \ln\left(1+\frac{\beta x}{1-x}\right).$$

2.4 Additional Functional Properties

Proposition 5 (Odds and Mills Ratios). *The UILxD has the following distinctive ratios:*

- ***Odds ratio:***

$$OR(x;\lambda,\beta) = \frac{F(x;\lambda,\beta)}{S(x;\lambda,\beta)} = \left(1+\frac{\beta x}{1-x}\right)^{\lambda} - 1. \tag{10}$$

- ***Mills ratio:***

$$MR(x;\lambda,\beta) = \frac{S(x;\lambda,\beta)}{f(x;\lambda,\beta)} = \frac{(1-x)(1+(\beta-1)x)}{\lambda\beta}. \tag{11}$$

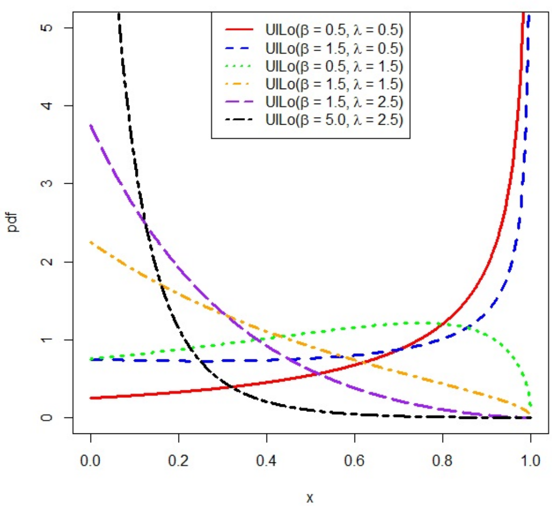

Figure 1. Pdf of UILxD with different values of λ and β.

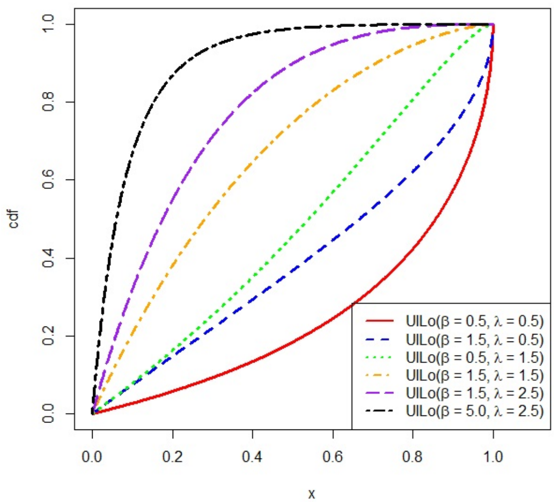

Figure 2. Cdf of UILxD with different values of λ and β.

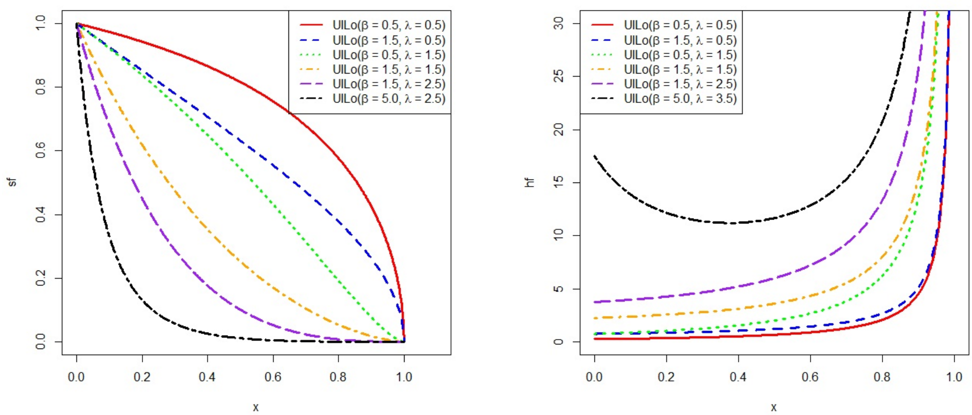

Figure 3. Survival and hazard rate functions of UILxD with different values of λ and β.

3. Important Properties of the Unit Inverse Lomax Distribution

This section presents key statistical properties of the Unit Inverse Lomax Distribution (UILxD), including its mode, quantile function, moments, shape characteristics, and order statistics. We also establish several novel propositions that highlight the distribution's unique behavior.

3.1 Mode of the Distribution

Proposition 6. *The Unit Inverse Lomax distribution is unimodal for all* $\lambda > 0$ *and* $\beta > 0$*. The mode is given by*

$$\mathrm{Mode}(X) = \begin{cases} x^* = \dfrac{\beta(\lambda+1)-2}{2(\beta-1)}, & 0 < \beta < 1,\ 1 < \lambda < \dfrac{2}{\beta} - 1, \\ \textit{at the boundary } (0 \textit{ or } 1), & \textit{otherwise.} \end{cases}$$

Proof. The probability density function is

$$f(x;\lambda,\beta) = \frac{\lambda\beta}{(1-x)^2}\left(1 + \frac{\beta x}{1-x}\right)^{-(\lambda+1)}, \qquad 0 < x < 1.$$

Taking the logarithmic derivative,

$$\frac{d}{dx}\log f(x) = \frac{1}{1-x}\left[2 - \frac{\beta(\lambda+1)}{1+(\beta-1)x}\right].$$

Setting this to zero yields the unique critical point

$$x^* = \frac{\beta(\lambda+1)-2}{2(\beta-1)},$$

provided $\beta \neq 1$.

The second derivative at x^* is

$$\frac{d^2}{dx^2}\log f(x^*) = \frac{\beta(\lambda+1)(\beta-1)}{(1-x^*)(1+(\beta-1)x^*)^2}.$$

- If $0 < \beta < 1$, then $\beta - 1 < 0$, so x^* is a local maximum whenever it lies in $(0,1)$. Solving $0 < x^* < 1$ under $\beta < 1$ gives $1 < \lambda < 2/\beta - 1$. This is the interior mode case.
- If $\beta > 1$, then $\beta - 1 > 0$, so any interior critical point would be a minimum. However, for $\beta > 1$, one can verify that $x^* \notin (0,1)$; hence no interior critical point exists, and the density is monotone decreasing, so the mode is at $x = 0$.
- If $\beta = 1$, the density reduces to $f(x;\lambda,1) = \lambda(1-x)^{\lambda-1}$, which is monotone decreasing for $\lambda > 1$ (mode at 0), increasing for $0 < \lambda < 1$ (mode at 1), and constant for $\lambda = 1$ (every point is a mode).

In all cases where the interior mode conditions are not satisfied, the mode occurs at a boundary point 0 or 1. Thus, the distribution is unimodal for all $\lambda > 0$, $\beta > 0$.

3.2 Quantile Function and Quartiles

Proposition 7 (Quantile Closure). *The quantile function* $Q(u;\lambda,\beta)$ *admits an explicit form:*

$$Q(u;\lambda,\beta) = \frac{(1-u)^{-1/\lambda} - 1}{(1-u)^{-1/\lambda} + \beta - 1}, \quad u \in (0,1). \tag{12}$$

Proof.

Let the cumulative distribution function be

$$F(x;\lambda,\beta) = 1 - \left(1 + \frac{\beta x}{1-x}\right)^{-\lambda}, \qquad 0 < x < 1,\ \lambda,\beta > 0.$$

To obtain the quantile function, set $F(x) = u$, where $0 < u < 1$:

$$u = 1 - \left(1 + \frac{\beta x}{1-x}\right)^{-\lambda}.$$

Rearranging,

$$\frac{\beta x}{1-x} = (1-u)^{-1/\lambda} - 1.$$

Solving for x,

$$\beta x = \left[(1-u)^{-1/\lambda} - 1\right](1-x),$$
$$x\left(\beta + (1-u)^{-1/\lambda} - 1\right) = (1-u)^{-1/\lambda} - 1.$$

Hence, the quantile function $Q(u) = F^{-1}(u)$ is

$$Q(u) = \frac{(1-u)^{-1/\lambda} - 1}{(1-u)^{-1/\lambda} + \beta - 1}, \qquad 0 < u < 1. \tag{13}$$

Corollary[Derived Quartiles]: The median (Q_2) and interquartile range (IQR) are given by:

$$Q_2 = \frac{2^{1/\lambda} - 1}{2^{1/\lambda} + \beta - 1}, \tag{14}$$

$$\mathrm{IQR} = \frac{4^{1/\lambda} - 1}{4^{1/\lambda} + \beta - 1} - \frac{\left(\frac{4}{3}\right)^{1/\lambda} - 1}{\left(\frac{4}{3}\right)^{1/\lambda} + \beta - 1}. \tag{15}$$

For ease of reference, the closed form expressions of the main distributional functions of the UILxD are summarized in Table 1.

Table 1. Closed form expressions of the Unit Inverse Lomax Distribution (UILxD)

Function	Expression
PDF	$f(x;\lambda,\beta) = \frac{\lambda\beta}{(1-x)^2}\left(1 + \frac{\beta x}{1-x}\right)^{-(\lambda+1)}, \quad x \in (0,1),$
CDF	$F(x;\lambda,\beta) = 1 - \left(1 + \frac{\beta x}{1-x}\right)^{-\lambda}, \quad x \in (0,1)$
Survival function	$S(x;\lambda,\beta) = \left(1 + \frac{\beta x}{1-x}\right)^{-\lambda}, \quad x \in (0,1)$
Hazard rate function	$h(x) = \frac{\lambda\beta}{(1-x)\left(1+(\beta-1)x\right)}, \quad x \in (0,1)$
Quantile function	$Q(u;\lambda,\beta) = \frac{(1-u)^{-1/\lambda}-1}{(1-u)^{-1/\lambda}+\beta-1}, \quad u \in (0,1).$

3.3 Moments and Shape Characteristics

Proposition 8 (Moment Existence)**.** *The r-th raw moment μ'_r exists for all $r \geq 1$ and is given by:*

$$\mu'_r = \lambda \sum_{k=0}^{\lfloor \lambda - r - 1 \rfloor} \binom{r+k-1}{k} (-1)^k \beta^{-(r+k)} \mathrm{B}(r+k+1, \lambda - r - k), \qquad r < \lambda - 1. \tag{16}$$

Proof.
Let X follow the Unit Inverse Lomax distribution, The r-th raw moment is defined as

$$\mu_r' = E[X^r] = \int_0^1 x^r f(x; \lambda, \beta)\, dx.$$

Substituting the pdf, we obtain

$$\mu_r' = \lambda\beta \int_0^1 \frac{x^r}{(1-x)^2} \left(1 + \frac{\beta x}{1-x}\right)^{-(\lambda+1)} dx.$$

Introduce the transformation

$$z = \frac{x}{1-x}, \qquad x = \frac{z}{1+z}, \qquad dx = \frac{dz}{(1+z)^2}.$$

Then

$$x^r = \frac{z^r}{(1+z)^r}, \qquad (1-x)^{-2} = (1+z)^2, \qquad 1 + \frac{\beta x}{1-x} = 1 + \beta z.$$

Substituting these into the integral yields

$$\begin{aligned} \mu_r' &= \lambda\beta \int_0^\infty \frac{z^r}{(1+z)^r} (1+z)^2 (1+\beta z)^{-(\lambda+1)} \frac{dz}{(1+z)^2} \\ &= \lambda\beta \int_0^\infty z^r (1+z)^{-r} (1+\beta z)^{-(\lambda+1)}\, dz. \end{aligned}$$

Using the generalized binomial expansion

$$(1+z)^{-r} = \sum_{k=0}^{\infty} \binom{r+k-1}{k} (-1)^k z^k, \qquad r > 0,$$

we write

$$z^r (1+z)^{-r} = \sum_{k=0}^{\infty} \binom{r+k-1}{k} (-1)^k z^{r+k}.$$

Substituting this expansion into the integral and interchanging summation and integration (justified by absolute convergence), we obtain

$$\mu_r' = \lambda\beta \sum_{k=0}^{\infty} \binom{r+k-1}{k} (-1)^k \int_0^\infty z^{r+k} (1+\beta z)^{-(\lambda+1)}\, dz.$$

Using the standard Beta-function identity

$$\int_0^\infty z^{a-1} (1+\beta z)^{-c}\, dz = \beta^{-a}\, \mathrm{B}(a, c-a), \qquad c > a > 0,$$

with $a = r + k + 1$ and $c = \lambda + 1$, we obtain

$$\int_0^\infty z^{r+k} (1+\beta z)^{-(\lambda+1)}\, dz = \beta^{-(r+k+1)} \mathrm{B}(r+k+1, \lambda - r - k),$$

which requires $\lambda - r - k > 0$.

The condition $\lambda - r - k > 0$ implies
$$k < \lambda - r.$$
Since k is a nonnegative integer, the summation is truncated at $k = \lfloor \lambda - r - 1 \rfloor$.

Substituting the integral result back into the summation gives the final expanded series form of the r-th raw moment:
$$\mu_r' = \lambda \sum_{k=0}^{\lfloor \lambda-r-1 \rfloor} \binom{r+k-1}{k} (-1)^k \beta^{-(r+k)} \mathrm{B}(r+k+1, \lambda-r-k), \qquad r < \lambda - 1.$$

Proposition 9 (Shape Measures)**.** *The Bowley skewness and Moors kurtosis are respectively:*
$$S_k = \frac{Q_3 - 2Q_2 + Q_1}{Q_3 - Q_1}, \tag{17}$$
$$K = \frac{(Q_{0.875} - Q_{0.625}) + (Q_{0.375} - Q_{0.125})}{Q_{0.75} - Q_{0.25}}, \tag{18}$$
where Q_p denotes the p-th quantile.

3.4 Order Statistics

Proposition 10 (Density of Order Statistics)**.** *For a random sample $X_1, \ldots, X_n$ from UILxD, the PDF of the r-th order statistic $X_{(r)}$ is:*
$$f_{r:n}(x) = C_{r:n} \frac{\lambda\beta}{(1-x)^2} \left(1 + \frac{\beta x}{1-x}\right)^{-\lambda(n-r+1)-1} \left[1 - \left(1 + \frac{\beta x}{1-x}\right)^{-\lambda}\right]^{r-1}, \tag{19}$$
where $C_{r:n} = \frac{n!}{(r-1)!(n-r)!}$.

Proof.

Let $X_1, X_2, \ldots, X_n$ be a random sample from the Unit Inverse Lomax distribution with parameters $\lambda > 0$ and $\beta > 0$. For a continuous distribution with pdf $f(x)$ and cdf $F(x)$, the pdf of the r-th order statistic $X_{(r)}$ is
$$f_{r:n}(x) = \frac{n!}{(r-1)!(n-r)!} [F(x)]^{r-1} [1 - F(x)]^{n-r} f(x), \qquad 0 < x < 1.$$

Substituting the UILxD cdf, we obtain
$$[F(x)]^{r-1} = \left[1 - \left(1 + \frac{\beta x}{1-x}\right)^{-\lambda}\right]^{r-1},$$
and
$$[1 - F(x)]^{n-r} = \left(1 + \frac{\beta x}{1-x}\right)^{-\lambda(n-r)}.$$

Combining these expressions yields
$$f_{r:n}(x) = \frac{n!}{(r-1)!(n-r)!} \frac{\lambda\beta}{(1-x)^2} \left(1 + \frac{\beta x}{1-x}\right)^{-(\lambda+1)} \left(1 + \frac{\beta x}{1-x}\right)^{-\lambda(n-r)} \times \left[1 - \left(1 + \frac{\beta x}{1-x}\right)^{-\lambda}\right]^{r-1}.$$

Simplifying the exponent of $\left(1+\dfrac{\beta x}{1-x}\right)$, we obtain

$$-(\lambda+1)-\lambda(n-r)=-\left[\lambda(n-r+1)+1\right].$$

Therefore, the pdf of the r-th order statistic is

$$f_{r:n}(x)=C_{r:n}\frac{\lambda\beta}{(1-x)^2}\left(1+\frac{\beta x}{1-x}\right)^{-\lambda(n-r+1)-1}\left[1-\left(1+\frac{\beta x}{1-x}\right)^{-\lambda}\right]^{r-1},\qquad 0<x<1,$$

where $C_{r:n}=\frac{n!}{(r-1)!(n-r)!}$.

Corollary 1 (Extreme Value Behavior). *Let $X_1,\ldots,X_n$ be a random sample from the Unit Inverse Lomax distribution with parameters $\lambda>0$ and $\beta>0$.*

(i) The minimum $X_{(1)}$ has a bounded density near $x=0$. In particular,

$$f_{1:n}(x)\to n\lambda\beta\quad \text{as } x\to 0^+.$$

(ii) The maximum $X_{(n)}$ satisfies

$$f_{n:n}(x)\sim n\lambda\beta^{-\lambda}(1-x)^{\lambda-1}\quad \text{as } x\to 1^-.$$

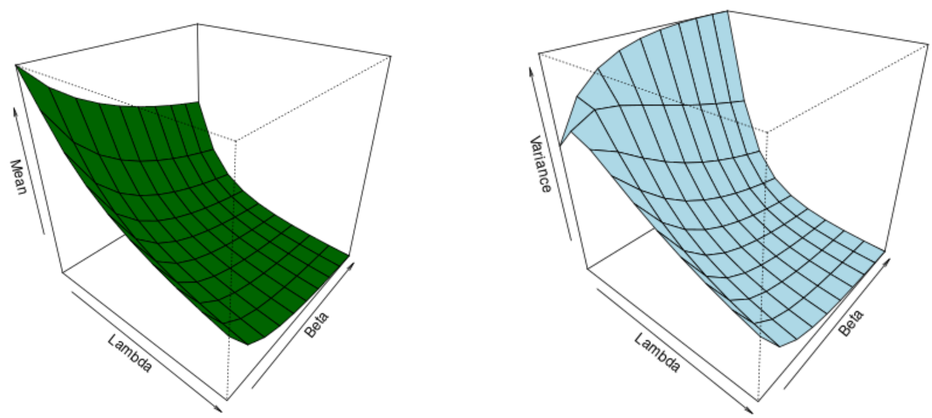

Figure 4. Mean and variance of UILxD with different values of λ and β.

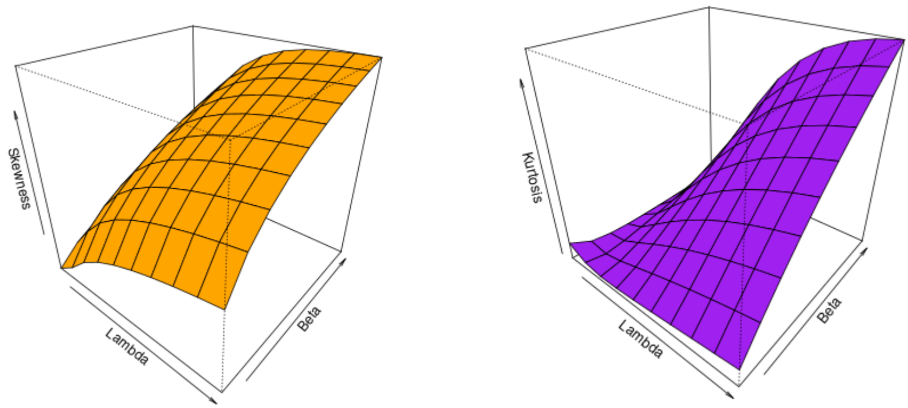

Figure 5. Skewness and kurtosis of UILxD with different values of λ and β.

4. Measures of uncertainty

Entropy is a basic term in data analysis that is used to quantify the degree of uncertainty or unpredictability in a dataset. It gives us a numerical representation of the information content in the data, enabling us to recognize and examine any hidden patterns or structures. We have derived the various entropy measures here.

4.1 Renyi entropy

The equation of renyi entropy is:

$$R_k(\lambda,\beta) = \frac{1}{1-k}\left[log\int_0^1 f(z;\lambda,\beta)^k dz\right],$$

$$= \frac{1}{1-k}\left[log\int_0^1 \frac{(\lambda\beta)^k}{(1-z)^{2k}}(1+\frac{\beta z}{1-z})^{-(\lambda+1)k}dz\right],$$

substitute $u = \frac{\beta z}{1-z}$, we get,

$$R_k(\lambda,\beta) = \frac{1}{1-k}\left[log(\lambda^k\beta^{k-1}\int_0^\infty \frac{1}{(1-\frac{u}{u+\beta})^{2k}}(1+u)^{-k(\lambda+1)}(1-\frac{u}{u+\beta})^2 du)\right],$$

$$= \frac{1}{1-k}\left[log(\lambda^k\beta^{k-1}\sum_{i=0}^{\infty}\binom{k(\lambda+1)+i-1}{i}\int_0^\infty (1-\frac{u}{u+\beta})^{2-2k}u^i du)\right],$$

$$= \frac{1}{1-k}\left[log(\lambda^k\beta^{1-k}\sum_{i=0}^{\infty}\binom{k(\lambda+1)+i-1}{i}\int_0^\infty \frac{u^i}{(u+\beta)^{2-2k}}du)\right],$$

$$R_k(\lambda,\beta) = \frac{1}{1-k}[log(\lambda^k\beta^{1-k}\sum_{i=0}^{\infty}\binom{k(\lambda+1)+i-1}{i}\eta)]. \tag{20}$$

Where,

$$\eta_{i,2-2k} = \int_0^\infty \frac{u^i}{(u+\beta)^{2-2k}}du.$$

Table 2. Mean, Variance, Skewness, and Kurtosis for Different Combinations of λ and β

λ	β	Mean	Variance	Skewness	Kurtosis
0.1	0.1	0.3454	0.1348	1.6957	2.9028
	0.2	0.3738	0.1288	1.6339	2.7159
	0.3	0.3868	0.1248	1.6078	2.6498
0.2	0.6	0.5913	0.0789	0.9445	1.8494
	0.8	0.5872	0.0804	0.8604	1.8552
	0.9	0.5847	0.0814	0.8268	1.8555
0.3	0.1	0.6833	0.0570	0.9444	1.7251
	0.2	0.6949	0.0543	0.5873	1.9911
	0.3	0.6920	0.0567	0.3629	2.1250
0.5	0.5	0.7089	0.0677	-0.6969	2.7037
	1.0	0.6351	0.0855	-0.3951	2.0095
	1.5	0.5854	0.0942	-0.1998	1.7730
1.0	0.5	0.6117	0.0777	-0.4692	2.0862
	1.0	0.4990	0.0828	0.0104	1.8036
	1.5	0.4321	0.0810	0.2917	1.9060
1.5	3.0	0.2301	0.0441	1.2357	3.9490
	3.5	0.2102	0.0403	1.3795	4.4571
	4.0	0.1939	0.0370	1.5097	4.9670
2.5	4.0	0.1145	0.0147	2.0395	8.1990
	4.5	0.1047	0.0130	2.1772	9.1116
	5.0	0.0964	0.0115	2.3055	10.0259
3.0	0.5	0.3645	0.0538	0.3480	2.1609
	1.0	0.2500	0.0373	0.8736	3.1180
	1.5	0.1935	0.0275	1.2098	4.1655
4.5	4.0	0.0610	0.0042	2.3556	11.1570
	4.5	0.0550	0.0035	2.4709	12.1739
	5.0	0.0501	0.0030	2.5755	13.1559
5.0	0.5	0.2631	0.0355	0.6847	2.7296
	1.0	0.1667	0.0197	1.2040	4.2492
	1.5	0.1232	0.0127	1.5277	5.6663

4.2 Exponential entropy

The equation of exponential entropy is,

$$E_k(\lambda, \beta) = \left[\int_0^1 f(z; \lambda, \beta)^k dz\right]^{\frac{1}{1-k}},$$

simplifying, we get,

$$E_k(\lambda, \beta) = \lambda^{\frac{k}{1-k}} \beta \left[\sum_{i=0}^{\infty} \binom{k(\lambda + 1) + i - 1}{i} \eta_{i,2-2k}\right]^{k-1}. \tag{21}$$

4.3 Havrada and Charvat entropy

The equation of Havrada and Charvat entropy is,

$$HC_k(\lambda, \beta) = \frac{1}{2^{1-k} - 1} \left[\int_0^1 f(z; \lambda, \beta)^k dz - 1\right],$$

$$HC_k(\lambda, \beta) = \frac{1}{2^{1-k} - 1} \left[\lambda^k \beta^{1-k} \sum_{i=0}^{\infty} \binom{k(\lambda + 1) + i - 1}{i} \eta_{i,2-2k} - 1\right]. \tag{22}$$

4.4 Arimoto entropy

The Arimoto entropy of UILxD is given by,

$$A_k(\lambda, \beta) = \frac{k}{1 - k} \left[(\int_0^1 f(z; \lambda, \beta)^k dz)^{\frac{1}{k}} - 1\right],$$

$$A_k(\lambda, \beta) = \frac{k}{1 - k} \left[\lambda^k \beta^{\frac{1-k}{k}} (\sum_{i=0}^{\infty} \binom{k(\lambda + 1) + i - 1}{i} \eta_{i,2-2k})^{\frac{1}{k}} - 1\right]. \tag{23}$$

4.5 Tsalli's entropy

The Tsalli's entropy of UILxD is given by,

$$T_k(\lambda, \beta) = \frac{1}{k - 1} \left[1 - \int_0^1 f(z; \lambda, \beta)^k dz)^k\right],$$

implies,

$$T_k(\lambda, \beta) = \frac{1}{k - 1} \left[1 - \lambda^k \beta^{1-k} \sum_{i=0}^{\infty} \binom{k(\lambda + 1) + i - 1}{i} \eta_{i,2-2k}\right]. \tag{24}$$

5. Estimation

The parameters of the UILxD λ and β, can be estimated using several estimation techniques. In this section, different estimation methods are considered to obtain the estimates of the model parameters. These methods include the Maximum Likelihood Estimation, Cramer Von Mises Estimation, Ordinary Least Squares Estimation, Weighted Least Squares Estimation, and Percentile Estimation. The performance of these estimators is later compared through a simulation study.

5.1 Maximum likelihood estimation

Let $X_1, X_2, ..., X_n$ be a random sample of size n drawn from a UILxD with parameters λ and β. The likelihood function of UILxD is given by,

$$L(\lambda,\beta) = \prod_{i=1}^{n} \frac{\lambda\beta}{(1-x_i)^2}\left(1+\frac{\beta x_i}{1-x_i}\right)^{-(\lambda+1)},$$

Taking logarithm,

$$logL(\lambda,\beta) = nlog\lambda + nlog\beta - 2\sum_{i=1}^{n} log(1-x_i) - (\lambda+1)\sum_{i=1}^{n} log\left(1+\frac{\beta x_i}{1-x_i}\right),$$

Then,

$$\frac{\partial}{\partial\lambda}\log(L(\lambda,\beta)) = 0,$$

implies,

$$\hat{\lambda} = n\left[\sum_{i=1}^{n} log\left(1+\frac{\beta x_i}{1-x_i}\right)\right]^{-1}. \tag{25}$$

Also,

$$\frac{\partial}{\partial\beta}\log(L(\lambda,\beta)) = 0,$$

implies,

$$\frac{n}{\beta} - (\lambda+1)[\sum_{i=1}^{n}\frac{x_i}{1-x_i+\beta x_i}] = 0. \tag{26}$$

Since the score equation for β is nonlinear, it does not admit a closed form solution. Therefore, the maximum likelihood estimators must be obtained numerically using iterative methods.

5.2 Cramer Von Mises minimum distance estimation

Let $X_1, X_2, \ldots, X_n$ be a random sample from the UILxD and $X_{(1)}, X_{(2)}, \ldots, X_{(n)}$ denote the corresponding order statistics. The Cramer Von Mises estimators (CvM) are obtained by minimizing the objective function

$$C(\lambda,\beta) = \frac{1}{12n} + \sum_{i=1}^{n}\left[F(x_{(i)} \mid \lambda,\beta) - \frac{2i-1}{2n}\right]^2,$$

where $x_{(i)}$ denotes the i-th order statistic and $F(\cdot)$ is the CDF of the UILxD. The objective function becomes

$$C(\lambda,\beta) = \frac{1}{12n} + \sum_{i=1}^{n}\left[1-\left(1+\frac{\beta x_{(i)}}{1-x_{(i)}}\right)^{-\lambda} - \frac{2i-1}{2n}\right]^2.$$

The CvM estimators of λ and β are obtained by minimizing $C(\lambda,\beta)$ with respect to the parameters. Since the objective function is nonlinear, numerical optimization techniques are required.

5.3 Ordinary and Weighted Least Squares Estimation

Let $X_1, X_2, \ldots, X_n$ be a random sample from the UILxD and $X_{(1)}, X_{(2)}, \ldots, X_{(n)}$ denote the corresponding order statistics.

Ordinary Least Squares Estimation: The Least Squares Estimators (LSEs) of λ and β are obtained by minimizing

$$S(\lambda, \beta) = \sum_{i=1}^{n} \left[F(x_{(i)} \mid \lambda, \beta) - \frac{i}{n+1} \right]^2.$$

Substituting the CDF of the UILxD, we obtain

$$S(\lambda, \beta) = \sum_{i=1}^{n} \left[1 - \left(1 + \frac{\beta x_{(i)}}{1 - x_{(i)}} \right)^{-\lambda} - \frac{i}{n+1} \right]^2.$$

Weighted Least Squares Estimation: The Weighted Least Squares (WLS) estimators are obtained by minimizing

$$W(\lambda, \beta) = \sum_{i=1}^{n} w_i \left[F(x_{(i)} \mid \lambda, \beta) - \frac{i}{n+1} \right]^2,$$

where

$$w_i = \frac{(n+1)^2(n+2)}{i(n-i+1)},$$

which are the reciprocals of the variances of the order statistics under the uniform distribution. Substituting the UILxD CDF, we obtain

$$W(\lambda, \beta) = \sum_{i=1}^{n} \frac{(n+1)^2(n+2)}{i(n-i+1)} \left[1 - \left(1 + \frac{\beta x_{(i)}}{1 - x_{(i)}} \right)^{-\lambda} - \frac{i}{n+1} \right]^2.$$

Since these objective functions are nonlinear in λ and β, the estimators are obtained numerically.

5.4 PC estimation

Within the framework of order statistics, represented as $X_{(1)} < X_{(2)} < \cdots < X_{(n)}$, the PC estimation method identifies the parameters λ and β by minimizing the corresponding expression with respect to these parameters.

$$P(\lambda, \beta) = \sum_{i=1}^{n} \left[x_{(i)} - Q\left(\frac{i}{n+1}; \lambda, \beta \right) \right]^2$$

implies,

$$P(\lambda, \beta) = \sum_{i=1}^{n} \left[x_{(i)} - \frac{(1 - \frac{i}{n+1})^{-1/\lambda} - 1}{(1 - \frac{i}{n+1})^{-1/\lambda} + \beta - 1} \right]^2. \tag{27}$$

6. Simulation Study

A Monte Carlo simulation study was conducted to assess the finite sample performance of the proposed estimators across various sample sizes, namely $n = 50, 100, 250, 500$, and 1000. For each scenario, the bias and mean squared error (MSE) were computed based on 1000 replications generated from the UILxD model with true parameter values $\lambda = 1$ and $\beta = 2$. As shown in Table 3, both the bias and MSE for all estimation methods decrease systematically as the sample size increases, providing empirical evidence of the consistency of the estimators. Among the competing methods, the MLE and WLSE generally exhibit the smallest MSEs, particularly for moderate to large sample sizes. Although the CVME and OLSE display relatively larger variability in small samples ($n = 50$), their performance improves noticeably as the sample size increases and stabilizes for $n \geq 250$. The PCE demonstrates competitive performance throughout and shows substantial improvement in estimation accuracy as the sample size grows. Overall, the simulation results indicate that the proposed estimators possess desirable finite sample properties and strong asymptotic behavior.

Table 3. Simulation results for different sample sizes when $\lambda = 1$ and $\beta = 2$

n	Measure	MLE	CVME	OLSE	WLSE	PCE
50	$\hat{\lambda}$	1.2200	1.4194	1.2041	1.1567	1.0757
	$\hat{\beta}$	1.9952	2.1450	2.4327	2.2739	2.3994
	MSE($\hat{\lambda}$)	0.4898	3.7808	1.5012	0.3840	0.1930
	MSE($\hat{\beta}$)	1.1401	1.8307	2.4004	1.7596	2.2031
	Bias($\hat{\lambda}$)	0.2200	0.4194	0.2041	0.1567	0.0757
	Bias($\hat{\beta}$)	-0.0048	0.1450	0.4327	0.2739	0.3994
100	$\hat{\lambda}$	1.0607	1.1004	1.0468	1.0427	1.0133
	$\hat{\beta}$	2.0971	2.1299	2.2685	2.1999	2.3002
	MSE($\hat{\lambda}$)	0.0688	0.1355	0.1048	0.0756	0.0642
	MSE($\hat{\beta}$)	0.6597	0.9950	1.1494	0.8840	1.0619
	Bias($\hat{\lambda}$)	0.0607	0.1004	0.0468	0.0427	0.0133
	Bias($\hat{\beta}$)	0.0971	0.1299	0.2685	0.1999	0.3002
250	$\hat{\lambda}$	1.0262	1.0351	1.0164	1.0190	1.0081
	$\hat{\beta}$	1.9994	2.0271	2.0793	2.0415	2.0721
	MSE($\hat{\lambda}$)	0.0192	0.0373	0.0340	0.0249	0.0236
	MSE($\hat{\beta}$)	0.2076	0.3106	0.3286	0.2599	0.2668
	Bias($\hat{\lambda}$)	0.0262	0.0351	0.0164	0.0190	0.0081
	Bias($\hat{\beta}$)	-0.0006	0.0271	0.0793	0.0415	0.0721
500	$\hat{\lambda}$	1.0076	1.0115	1.0025	1.0038	0.9972
	$\hat{\beta}$	2.0102	2.0237	2.0496	2.0305	2.0544
	MSE($\hat{\lambda}$)	0.0086	0.0153	0.0147	0.0107	0.0113
	MSE($\hat{\beta}$)	0.0914	0.1407	0.1453	0.1118	0.1257
	Bias($\hat{\lambda}$)	0.0076	0.0115	0.0025	0.0038	-0.0028
	Bias($\hat{\beta}$)	0.0102	0.0237	0.0496	0.0305	0.0544
1000	$\hat{\lambda}$	1.0059	1.0062	1.0018	1.0038	1.0011
	$\hat{\beta}$	2.0148	2.0264	2.0393	2.0259	2.0349
	MSE($\hat{\lambda}$)	0.0041	0.0071	0.0070	0.0050	0.0054
	MSE($\hat{\beta}$)	0.0520	0.0802	0.0818	0.0635	0.0694
	Bias($\hat{\lambda}$)	0.0059	0.0062	0.0018	0.0038	0.0011
	Bias($\hat{\beta}$)	0.0148	0.0264	0.0393	0.0259	0.0349

7. Data Analysis

Here, we analyze three datasets:

1. **Snowfall data**: 30 daily measurements (inches of water) from unseeded experiments in Climax, Colorado (Mielke *et al.*, 1971): 0.030, 0.020, 0.015, 0.045, 0.100, 0.100, 0.125, 0.190, 0.390, 0.110, 0.070, 0.010, 0.055, 0.220, 0.080, 0.005, 0.125, 0.035, 0.085, 0.060, 0.010, 0.065, 0.020, 0.260, 0.030, 0.015, 0.025, 0.010, 0.495, 0.085.
2. **Tensile strength**: 30 polyester fiber measurements (Mazucheli *et al.*, 2019b): 0.023, 0.032, 0.054, 0.069, 0.081, 0.094, 0.105, 0.127, 0.148, 0.169, 0.188,0.216, 0.255, 0.277, 0.311, 0.361, 0.376, 0.395, 0.432, 0.463, 0.481, 0.519,0.529, 0.567, 0.642, 0.674, 0.752, 0.823, 0.887, 0.926.
3. **Capacity factors**: SC16 algorithm outputs (Altun & Hamedani, 2018): 0.809, 0.717, 0.544, 0.492, 0.403, 0.344, 0.213, 0.116, 0.116, 0.092, 0.070, 0.059, 0.048, 0.036, 0.029, 0.021, 0.014, 0.011, 0.008, 0.006.

To establish UILxD's superiority, we conduct a comprehensive comparison with six established unit interval distributions:

1. Beta (BD):

$$f(x) = \frac{x^{\alpha-1}(1-x)^{\beta-1}}{B(\alpha,\beta)}, \quad 0 < x < 1. \tag{28}$$

2. Kumaraswamy (KD):

$$f(x) = \alpha\beta x^{\alpha-1}(1-x^{\alpha})^{\beta-1}, \quad 0 < x < 1. \tag{29}$$

3. Unit Inverse Weibull (UIWD):

$$f(x) = \alpha\beta x^{-2}\left(\tfrac{1}{x}-1\right)^{-\beta-1} e^{-\alpha\left(\frac{1}{x}-1\right)^{-\beta}}, \quad 0 < x < 1. \tag{30}$$

4. Unit Inverse Exponentiated Weibull (UIEW):

$$f(x) = \alpha\beta\delta x^{-1}(-\log x)^{-\alpha-1} e^{-\beta(-\log x)^{-\alpha}}\left(1-e^{-\beta(-\log x)^{-\alpha}}\right)^{\delta-1}, \quad 0 < x < 1. \tag{31}$$

5. Unit Lindley (ULD):

$$f(x) = \frac{\theta^2}{1+\theta}\,\frac{1}{(1-x)^3}\exp\left(-\frac{\theta x}{1-x}\right), \quad 0 < x < 1,\ \theta > 0. \tag{32}$$

6. Unit Birnbaum–Saunders (UBSD):

$$f(x) = \frac{1}{2\alpha\beta\sqrt{2\pi}}\left[\left(-\frac{\beta}{\log x}\right)^{1/2} + \left(-\frac{\beta}{\log x}\right)^{3/2}\right]\exp\left[\frac{1}{2\alpha^2}\left(\frac{\log x}{\beta}+\frac{\beta}{\log x}+2\right)\right], \quad 0 < x < 1. \tag{33}$$

Our comparative analysis employs established statistical metrics to evaluate model performance. For model selection, we utilize four information criteria: the Akaike Information Criterion (AIC) , the Bayesian Information Criterion (BIC) , the corrected AIC (AICc) , and the Hannan Quinn Information Criterion (HQIC) . Goodness of fit is assessed through the Kolmogorov-Smirnov (KS) test. These criteria collectively evaluate each distribution's parsimony, fit quality, and predictive accuracy while accounting for model complexity relative to sample size.

Table 4. Complete Goodness of Fit Metrics Comparison (Three Datasets)

Distribution	Parameters	AIC	AICc	BIC	HQIC	KS (p-value)
		Data 1 (n = 30)				
UILxD	$\lambda = 2.2273,\ \beta = 5.9705$	**-77.621**	**-77.176**	**-74.818**	**-76.724**	**0.0889 (0.972)**
BD	$\alpha = 0.8576,\ \beta = 7.8057$	-75.122	-74.677	-72.319	-74.225	0.1287 (0.703)
UIWD	$\alpha = 5.6783,\ \beta = 0.7936$	-74.665	-74.220	-71.862	-73.768	0.2338 (0.075)
KD	$\alpha = 0.8615,\ \beta = 6.8358$	-75.595	-75.151	-72.793	-74.699	0.1208 (0.774)
UIEW	α=0.2359,β=15.0736, δ=90428.8	-77.209	-76.286	-73.005	-75.864	0.5884 (1.90e-9)
ULD	$\theta = 8.4300$	-72.7696	-72.6267	-71.3684	-72.3210	0.4944 (8.53e-7)
UBSD	$\alpha = 0.4818,\ \beta = 2.6307$	102.8476	103.2921	105.6500	103.7441	0.1456 (0.5473)
		Data 2 (n = 30)				
UILxD	$\lambda = 0.7137,\ \beta = 3.1471$	**-1.4168**	**-0.9724**	**1.3856**	**-0.5203**	**0.0798 (0.9829)**
BD	$\alpha = 0.7653,\ \beta = 0.9945$	1.7056	2.1500	4.5080	2.6021	0.1175 (0.7584)
UIWD	$\alpha = 0.7795,\ \beta = 0.3605$	21.5161	21.9606	24.3185	22.4126	0.9999 (1.22e-15)
KD	$\alpha = 0.7706,\ \beta = 1.0061$	1.7054	2.1498	4.5078	2.6019	0.1154 (0.7774)
UIEW	$\alpha = 0.2402,\ \beta = 2.4922,\ \delta = 10.0$	24.9349	25.8580	29.1385	26.2796	0.2140 (0.1101)
ULD	$\theta = 1.0503$	20.1704	20.3132	21.5716	20.6186	0.4491 (4.85e-6)
UBSD	$\alpha = 1.0772,\ \beta = 0.8483$	85.6973	86.1417	88.4997	86.5938	0.1613 (0.3753)
		Data 3 (n = 20)				
UILxD	$\lambda = 0.3660,\ \beta = 31.0742$	**-22.4862**	**-21.8862**	**-20.2152**	**-21.9150**	**0.0907 (0.9915)**
BD	$\alpha = 0.3879,\ \beta = 0.6025$	-15.1432	-14.5432	-12.8722	-14.5720	0.2098 (0.2632)
UIWD	$\alpha = 0.8710,\ \beta = 0.2915$	-9.7857	-9.1857	-7.5147	-9.2145	0.9985 (0.0000)
KD	$\alpha = 0.3747,\ \beta = 0.6695$	-14.3124	-13.7124	-12.0414	-13.7412	0.2184 (0.2225)
UIEW	$\alpha = 0.1919,\ \beta = 2.6072,\ \delta = 10.0$	3.1018	4.3649	6.5082	3.9585	0.2253 (0.1934)
ULD	$\theta = 2.3445$	-3.1713	-2.9491	-2.1756	-2.9769	0.6113 (6.43e-7)
UBSD	$\alpha = 0.9829,\ \beta = 1.6493$	81.1205	81.8265	83.1120	81.5093	0.2573 (0.1413)

The comprehensive comparison across three distinct datasets consistently demonstrates the superior performance of the UILxD. As reported in Table (4), UILxD attains the minimum AIC, AICc, BIC, and HQIC values in all cases, indicating an optimal balance between goodness of fit and model complexity. In addition, UILxD alone exhibits very small KS statistics with correspondingly high p-values (KS = 0.0889, p = 0.972; KS = 0.0798, p = 0.9829; KS = 0.0907, p = 0.9915), indicating an excellent fit to the data.

The fitted cumulative distribution functions (CDFs) for Datasets 1, 2, and 3 demonstrate that the UILxD model closely aligns with the empirical data, confirming its superior fit compared to alternative distributions. The near perfect overlap between the theoretical UILxD CDF and the observed data underscores its robustness in capturing the underlying statistical behavior. These results validate UILxD as the preferred choice for modeling this type of data due to its accuracy and reliability.

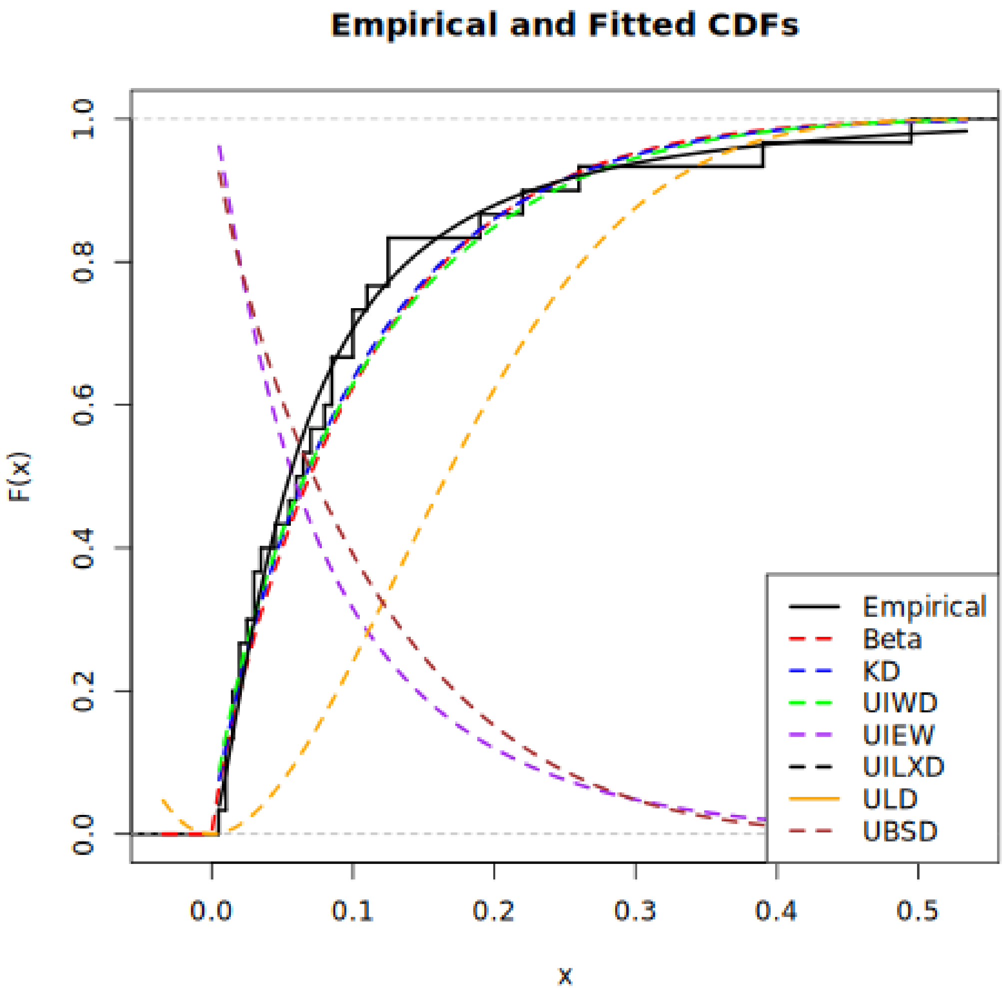

Figure 6. Estimated CDFs for the data 1.

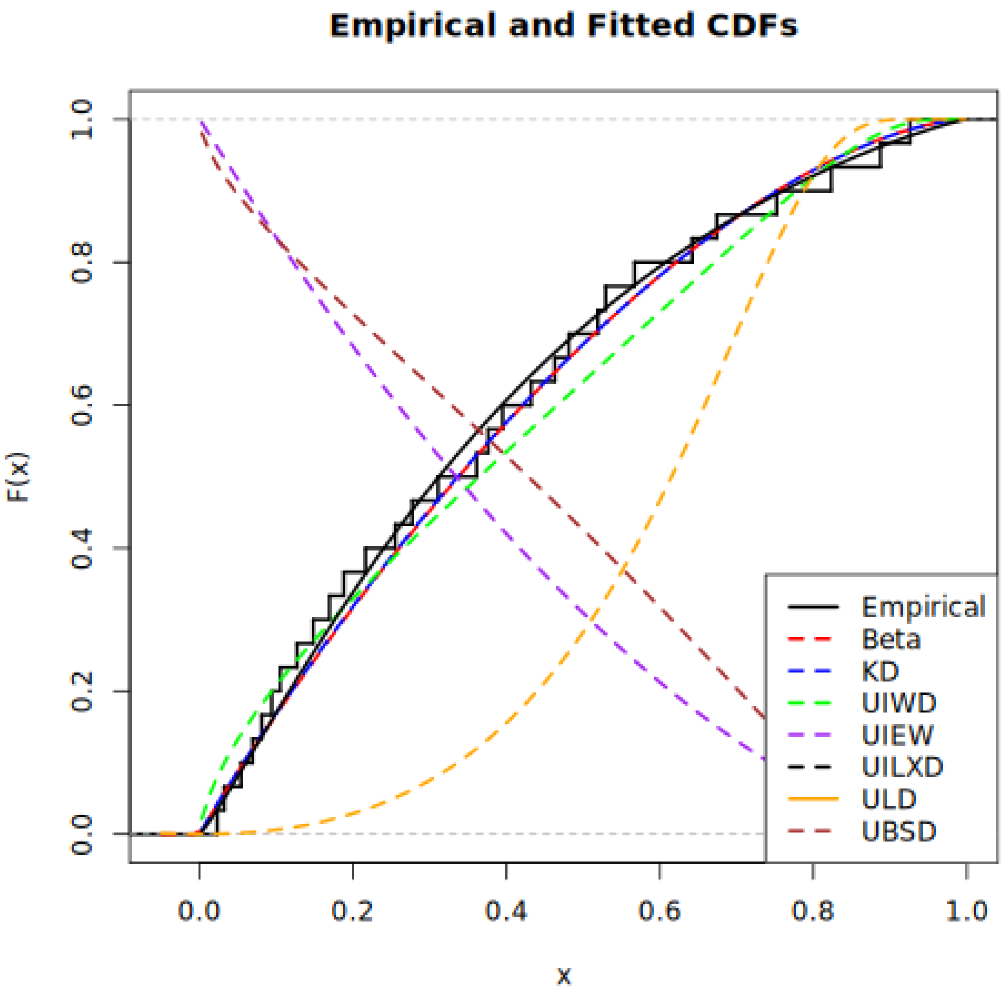

Figure 7. Estimated CDFs for the data 2.

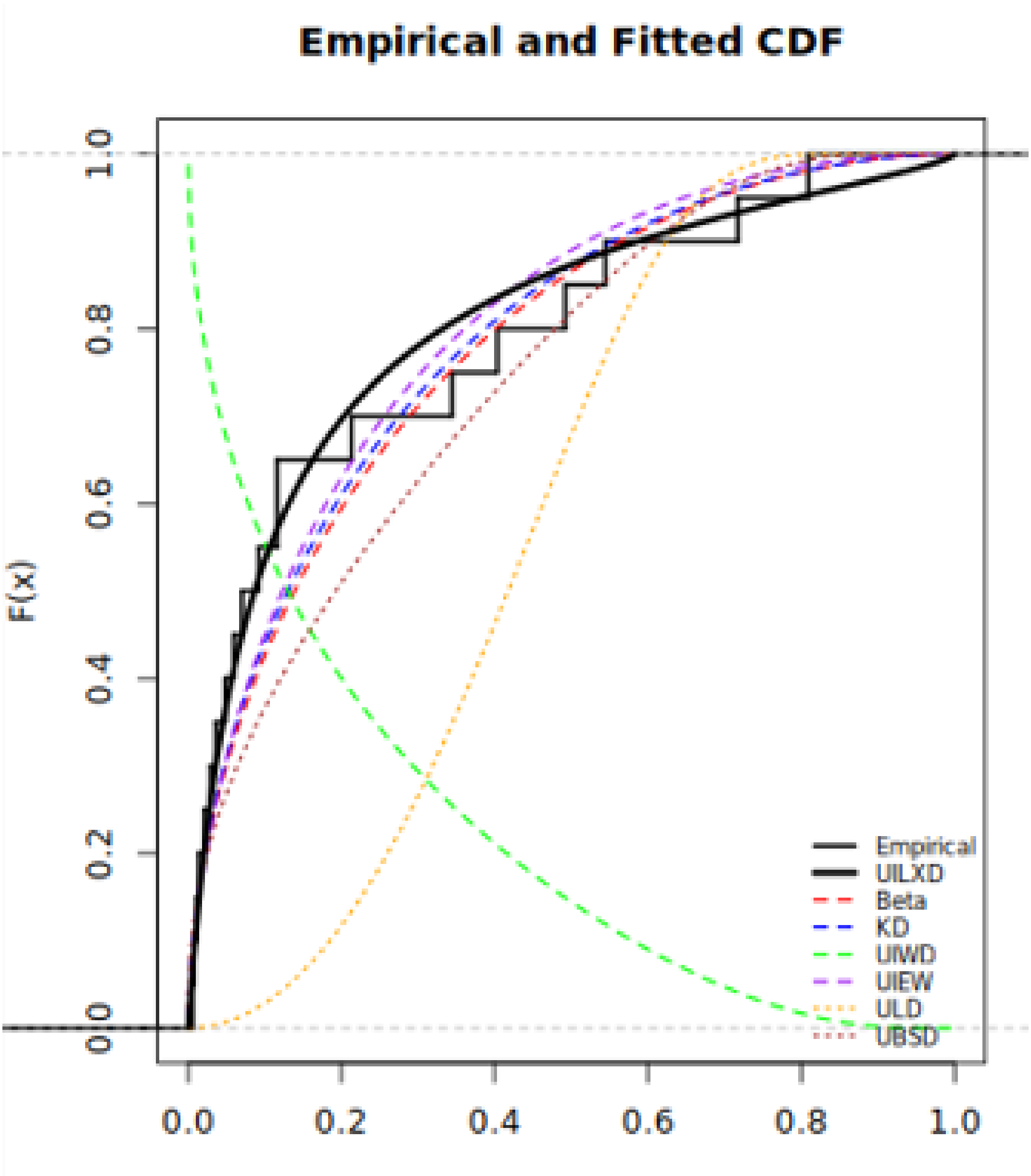

Figure 8. Estimated CDFs for the data 3.

8. Conclusion

The Unit Inverse Lomax Distribution (UILxD) emerges as a powerful and flexible statistical model for analyzing data within the unit interval (0,1). This study has comprehensively developed the theoretical framework of the UILxD, addressing closed form expressions for its PDF, CDF, survival function, hazard rate, and quantile function. These analytical forms, coupled with the distribution's ability to exhibit heavy tails and explosive growth near the upper boundary, distinguish it from traditional unit interval distributions like the Beta and Kumaraswamy distributions. The UILxD's unimodality, explicit quantile function, and derived moments—including skewness and kurtosis—demonstrate its flexibility in capturing a wide range of data shapes, from highly skewed to heavy tailed distributions.

A significant contribution of this work is the thorough exploration of the UILxD's measures of uncertainty, such as Renyi, Exponential, Havrada-Charvat, Arimoto, and Tsallis entropies. These measures provide valuable insights into the distribution's ability to quantify unpredictability in datasets, enhancing its applicability in information theoretic contexts. Furthermore, the study evaluates multiple parameter estimation methods—Maximum Likelihood Estimation, Cramer-Von Mises, Ordinary and Weighted Least Squares, and Percentile Estimation—through an extensive Monte Carlo simulation. The results reveal that MLE offers superior performance for estimating the shape parameter λ, while Weighted Least Squares excels for the scale parameter β in moderate to large samples, providing practical guidance for researchers based on sample size and parameter focus.

The practical utility of the UILxD is demonstrated through its application to three diverse real world datasets: snowfall measurements, tensile strength of polyester fibers, and capacity factors from the SC16 algorithm. Across all datasets, the UILxD consistently outperforms established unit interval distributions, achieving the lowest AIC, AICc, BIC, and HQIC values and the highest Kolmogorov-Smirnov p-values. This superior fit underscores the UILxD's robustness in modeling complex data patterns, particularly those with extreme values near boundaries, as seen in fields like reliability engineering, finance, and insurance.

In summary, the Unit Inverse Lomax Distribution stands as a robust and flexible tool for modeling unit interval data, offering a compelling alternative to existing distributions. Its well defined statistical properties, reliable estimation methods, and demonstrated superiority in real world applications position it as a valuable asset for researchers and practitioners across various domains. This work lays a strong foundation for future studies to build upon, potentially unlocking new avenues for statistical modeling and analysis.

Acknowledgments

The authors gratefully acknowledge the insightful comments from the anonymous reviewers and the editorial team of the Brazilian Journal of Biometrics. This work received no specific external funding.

Conflicts of Interest

The authors declare no conflict of interest.

Author Contributions

All authors contributed significantly to the development of this manuscript. **Conceptualization**: SHAMEERA, T.; BINDU, P. P. **Data curation**:SHAMEERA, T.; BINDU, P. P. **Formal analysis**: SHAMEERA, T.; BINDU, P. P.**Funding acquisition**:SHAMEERA, T.; BINDU, P. P. **Investigation**: SHAMEERA, T.; BINDU, P. P.**Methodology**: SHAMEERA, T.; BINDU, P. P.**Project administration**: SHAMEERA, T.; BINDU, P. P.**Software**: SHAMEERA, T.; BINDU, P. P.**Resources**: SHAMEERA, T.; BINDU, P. P.**Supervision**: SHAMEERA, T.; BINDU, P. P.**Validation**: SHAMEERA, T.; BINDU, P. P. **Visualization**: SHAMEERA, T.; BINDU, P. P.**Writing - original draft**: SHAMEERA, T.; BINDU, P. P. **Writing - review and editing**: SHAMEERA, T.; BINDU, P. P.

References

[1] Abiodun, A.A. & Ishaq, A.I. On Maxwell–Lomax distribution: properties and applications. *Arab Journal of Basic and Applied Sciences* **29**, 221–232 (2022). https://doi.org/10.1080/25765299.2022.2093033

[2] Altun, E. & Hamedani, G. The log-xgamma distribution with inference and application. *Journal de la Societe Francaise de Statistique* **159**, 40–55 (2018).

[3] Bantan, R.A.R., Jamal, F., Chesneau, C. & Elgarhy, M. Theory and applications of the unit Gamma/Gompertz distribution. *Mathematics* **9**, 1850 (2021). https://doi.org/10.3390/math9161850

[4] Bhatti, F.A., Ali, A., Hamedani, G., & Korkmaz, M.C. The unit generalized log Burr XII distribution: properties and application. *AIMS Mathematics* **6**, 10253–10265 (2021). https://www.aimspress.com/article/doi/10.3934/math.2021592

[5] Cordeiro, G.M., Ortega, E.M.M. & Popovic, B.V. The gamma-Lomax distribution. *Journal of Statistical Computation and Simulation* **85**, 305–319 (2013).

[6] El-bassiouny, H., Abdo, N.F. & Shahen, H.S. Exponential Lomax Distribution. *International Journal of Computer Applications* **121**, 24–29 (2012).

[7] Ferreira, A.B. & Mazucheli, J. The zero, one and zero-and-one-inflated New unit-Lindley distributions. *Brazilian Journal of Biometrics* **40**(3), 291–326 (2022). https://doi.org/10.28951/bjb.v40i3.571

[8] Gemeay, A.M., Alsadat, N., Chesneau, C. & Elgarhy, M. Power unit inverse Lindley distribution with different measures of uncertainty, estimation and applications. *AIMS Mathematics* **9**, 20976–21024 (2024). https://www.aimspress.com/article/doi/10.3934/math.20241021

[9] Ghitany, M.E., Mazucheli, J., Menezes, A.F.B. & Alqallaf, F. The unit-inverse Gaussian distribution: A new alternative to two-parameter distributions on the unit interval. *Communications in Statistics – Theory and Methods* **48**, 3423–3438 (2018).

[10] Hassan, A.S. & Abd-Allah, M. Exponentiated Weibull-Lomax Distribution: Properties and Estimation. *Journal of Data Science* **16**, 277–298 (2022).

[11] Hassan, A.S. & Alharbi, R.S. Different estimation methods for the unit inverse exponentiated Weibull distribution. *Communications for Statistical Applications and Methods* **30**, 191–213 (2023). https://doi.org/10.29220/CSAM.2023.30.2.191

[12] Hassan, A.S. & Mohamed, R.E. Weibull Inverse Lomax Distribution. *Pakistan Journal of Statistics and Operation Research* **15**, 587–603 (2019).

[13] Ishaq, A.I., Suleiman, A.A., Daud, H., Singh, N.S.S., Othman, M., Sokkalingam, R., Wiratchotisatian, P., Usman, A.G. & Abba, S.I. Log-Kumaraswamy distribution: its features and applications. *Frontiers in Applied Mathematics and Statistics* **9**, 1258961 (2023). https://doi.org/10.3389/fams.2023.1258961

[14] Kilany, N.M. Weighted Lomax distribution. *SpringerPlus* **5**, 1862 (2016).

[15] Korkmaz, M.C. & Chesneau, C. On the unit Burr-XII distribution with the quantile regression modeling and applications. *Computational and Applied Mathematics* **4**, 1–26 (2021). https://doi.org/10.1007/s40314-021-01418-5

[16] Kumaraswamy, P. A generalized probability density function for double-bounded random processes. *Journal of Hydrology* **46**, 79–88 (1980). https://doi.org/10.1016/0022-1694(80)90036-0

[17] Lemonte, A.J. & Cordeiro, G.M. An extended Lomax distribution. *Statistics* **47**, 800–816 (2011).

[18] Mazucheli, J., Menezes, A.F. & Dey, S. The unit Birnbaum-Saunders distribution with applications. *Chilean Journal of Statistics* **9**, 47–57 (2018).

[19] Mazucheli, J., Menezes, A.F.B. & Ghitany, M.E. The unit-Weibull distribution and associated inference. *Journal of Applied Probability and Statistics* **13**, 1–22 (2018). https://doi.org/10.1080/02664763.2019.1657813

[20] Mazucheli, J., Menezes, A.F.B. & Chakraborty, S. On the one-parameter unit Lindley distribution and its associated regression model for proportion data. *Journal of Applied Statistics* **46**, 700–714 (2019). https://doi.org/10.1080/02664763.2018.1511774

[21] Mazucheli, J., Menezes, A.F.B. & Dey, S. Unit-Gompertz distribution with applications. *STATISTICA* **79**, 25–43 (2019). https://doi.org/10.6092/issn.1973-2201/8497

[22] Mielke, P.W., Grant, L.O. & Chappell, C.F. An independent replication of the Climax wintertime orographic cloud seeding experiment. *Journal of Applied Meteorology* **10**, 1198–1212 (1971). https://doi.org/10.1175/1520-0450(1971)010%3C1198:AIROTC%3E2.0.CO;2

[23] Rady, E.H.A., Hassanein, W.A. & Elhaddad, T.A. The power Lomax distribution with an application to bladder cancer data. *SpringerPlus* **5**, 1838 (2016).

[24] Sakthivel, M. & Pandiyan, P. A New Model of Mixture Distribution Using a Survival Analysis of Cancer Patients. *Brazilian Journal of Biometrics* **43**(1), e-43733 (2025). https://doi.org/10.28951/bjb.v43i1.733

[25] Shameera, T. & Bindu, P.P. Exploring the adaptability of the unit inverse Weibull distribution for modeling data on the unit interval. *Reliability: Theory and Applications* **18**, 76 (2023).